Supplementary information

Information encrypted heterogeneous hydrogel with programmable mechanical properties enabled by 3D patterning

Yuhang Ye[†], *Zhengyang Yu*[†], *Yifan Zhang*, *Feng Jiang*[*]

Sustainable Functional Biomaterials Lab, Department of Wood Science, University of British Columbia, 2900 - 2424 Main Mall, Vancouver, BC V6T 1Z4, Canada.

[†] These two authors contribute equally.

*Corresponding author: Prof. Feng Jiang E-mail: feng.jiang@ubc.ca

Keywords: hydrogels; 3D printing; information encryption; cellulose nanofibrils; hydroxypropyl cellulose.

Figure S1. Rheology property of pure HPC (35 wt%), storage moduli (G′) and loss moduli (G′’) vs oscillation stress.

Figure S2. Rheology property of pure HPC (35 wt%): steady-state viscosity vs shear

Figure S3. Rheology property of pure CNF (2.2 wt%), storage moduli (G′) and loss moduli (G′’) vs oscillation stress.

Figure S4. Rheology property of pure CNF (2.2 wt%): steady-state viscosity vs shear rate.

Figure S5. Rheology property of HPC/CNF at varied ratios: oscillation stress vs Tan theta

Figure S6. Appearance change of HPC/CNF ink before and after ambient drying

Figure S7. Digital photos representing Patterned HPC-CNF materials at net structure after ambient drying; (f) Digital photos representing the deformation of HPC/CNF materials.

Figure S8. Digital photos demonstrating the weak mechanical property of HPC/CNF ink.

Figure S9. optical microscopic images representing the existence of crystallites under polarizer.

Figure S10. Optical images indicating the appearance change of patterned hydrogels during stretching process (under polarizer)

Figure S11. UV-vis spectrum of CNF, HPC, and CNF/HPC materials.

Figure S12. Optical photos recording the dual (swelling and heating) stimulated actuation behavior of patterned hydrogel at flower geometry.

Table S1. Commonly used methods for adjusting the LCST of HPC.

Table S2. Summary of previously reported information encryption hydrogels.

Video S1. video recording the great interfacial interaction between hydrogel and patterned phase at room temperature.

Video S2. video recording the great interfacial interaction between hydrogel and patterned phase at elevated temperature.

Video S3. video recording the mechanical deformation of patterned hydrogels upon being stretched under polarizer.

Video S4. video recording the instant responsive behavior of patterned hydrogels to heat.

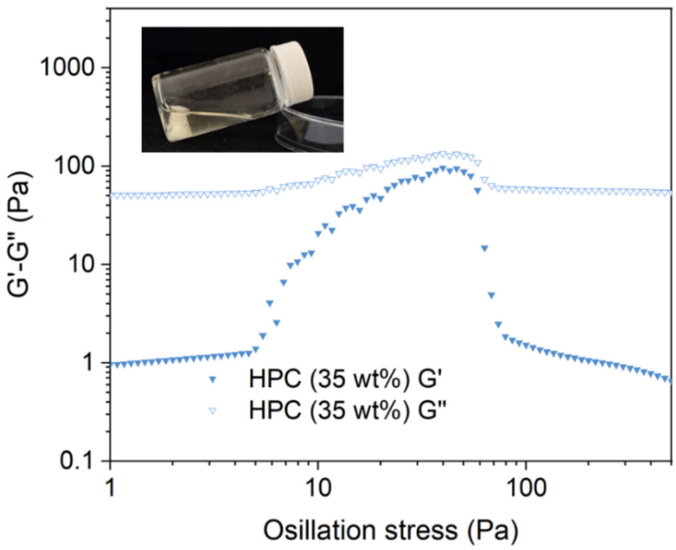

Figure S1. Rheology property of pure HPC (35 wt%), storage moduli (G′) and loss moduli (G′′) vs oscillation stress.

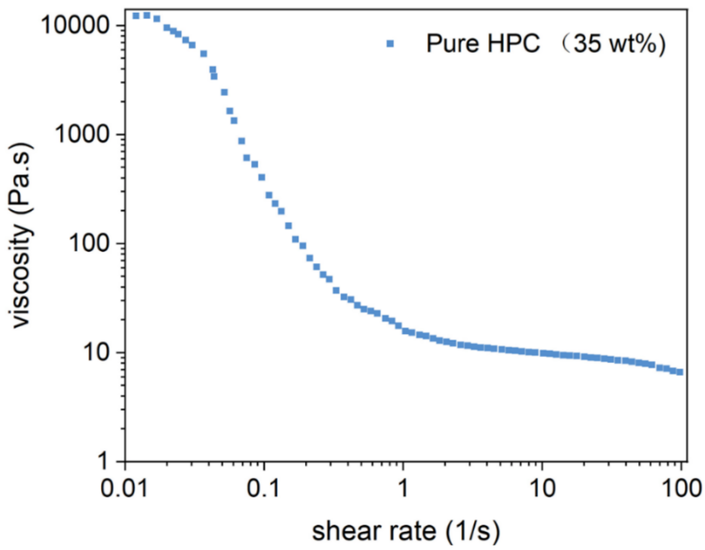

Figure S2. Rheology property of pure HPC (35 wt%): steady-state viscosity vs shear rate.

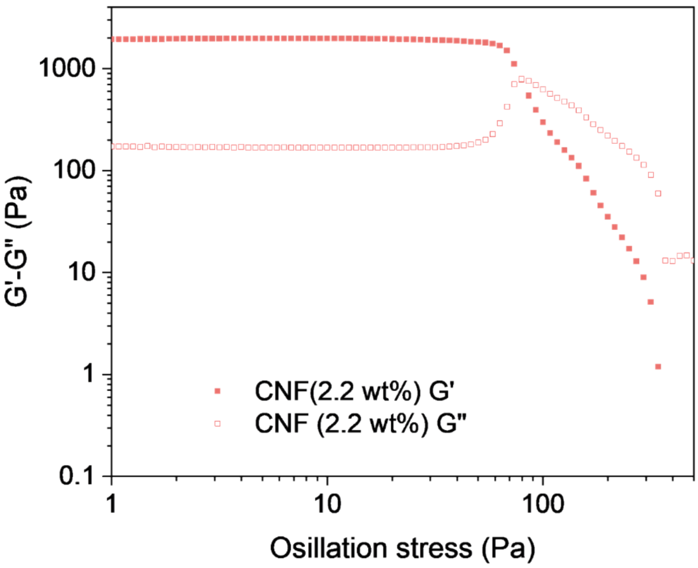

Figure S3. Rheology property of pure CNF (2.2 wt%), storage moduli (G′) and loss moduli (G′′) vs oscillation stress.

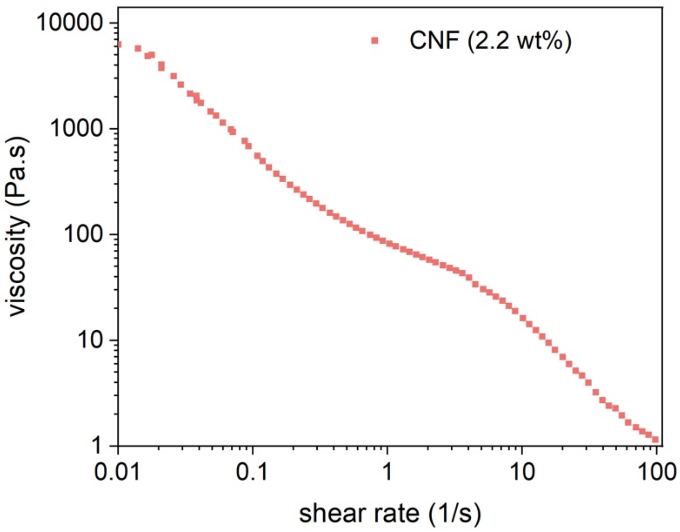

Figure S4. Rheology property of pure CNF (2.2 wt%): steady-state viscosity vs shear rate.

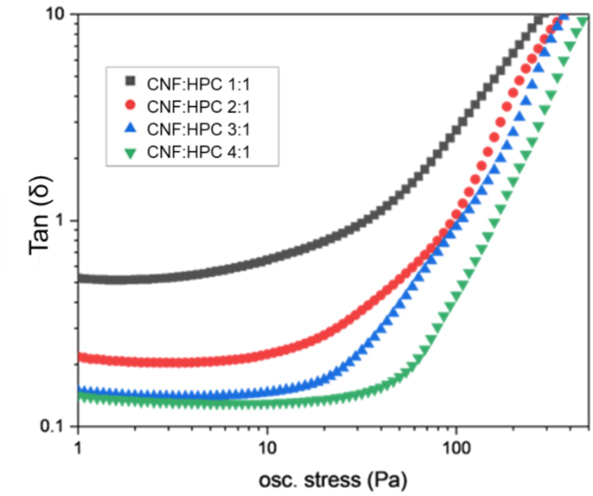

Figure S5. Rheology property of HPC/CNF at varied ratios: oscillation stress vs Tan theta

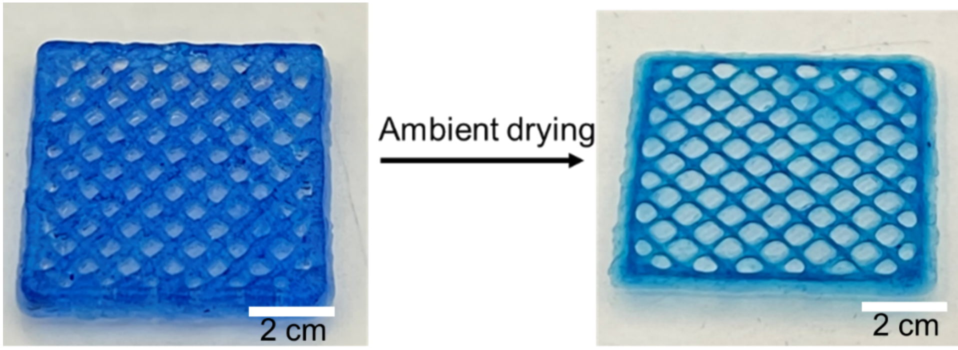

Figure S6. Appearance change of HPC/CNF ink before and after ambient drying

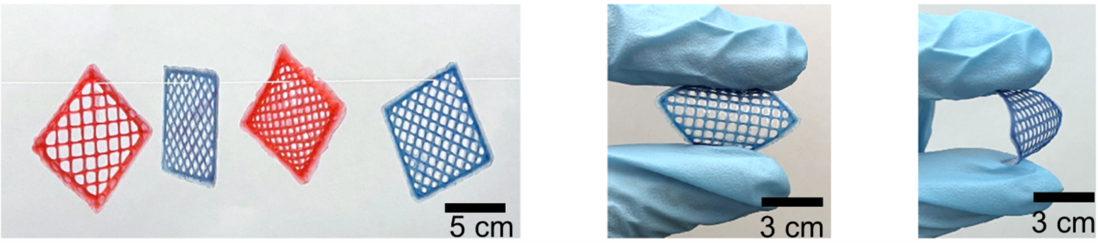

Figure S7 Digital photos representing (a) Patterned HPC-CNF materials at net structure after ambient drying; (b) representing the deformation of HPC/CNF materials.

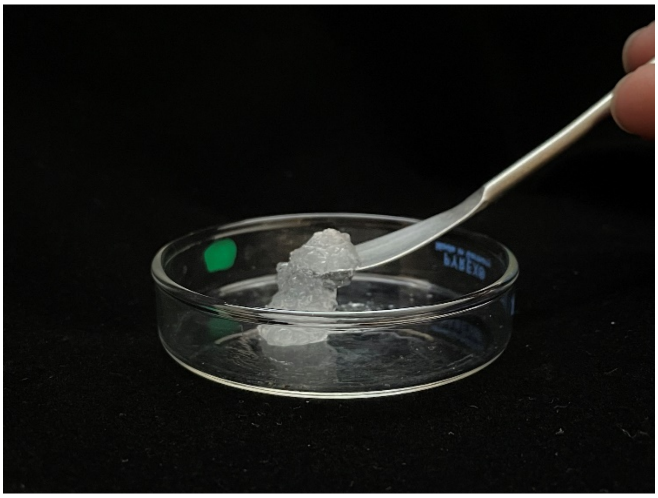

Figure S8 Digital photos demonstrating the weak mechanical property of HPC/CNF ink.

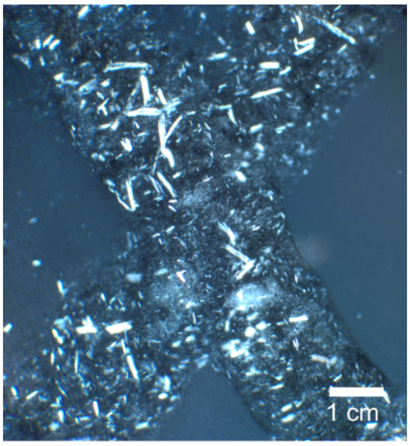

Figure S9 optical microscopic images representing the existence of crystallites under cross-polarized lenses.

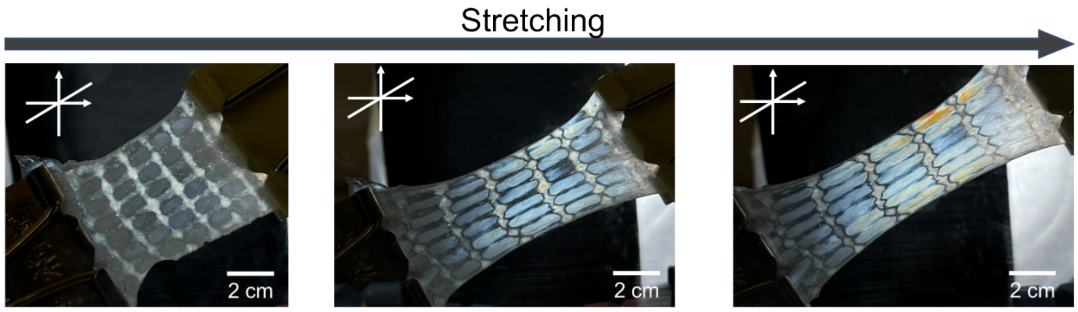

Figure S10. Optical images indicating the appearance change of patterned hydrogels during stretching process (under cross-polarized lenses)

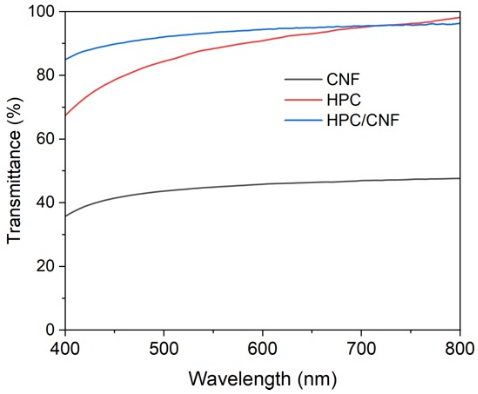

Figure S11. UV-vis spectrum of CNF, HPC, and CNF/HPC inks.

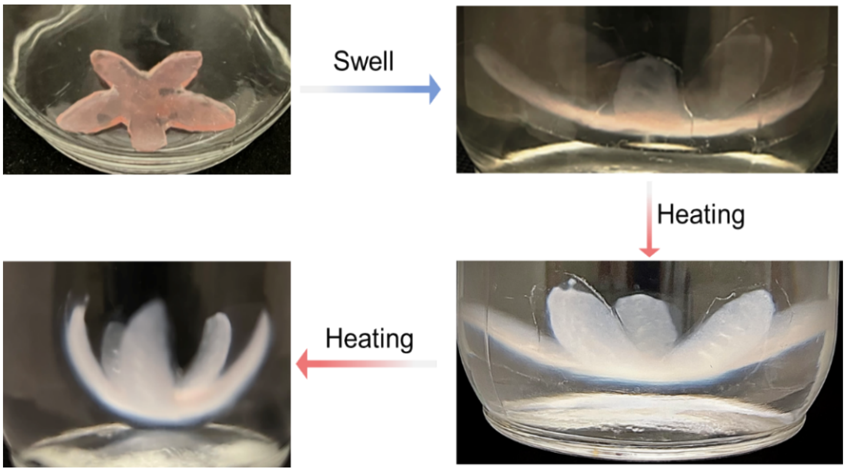

Figure S12 Optical photos recording the dual (swelling and heating) stimulated actuation behavior of patterned hydrogel at flower geometry.

Table S1 Commonly used methods for adjusting the LCST of HPC

No.	Methods	Experiment	LCST	Reference
1	Increasing molecular weight	From 80,000 to 370,000	Decreased from 46.2 to 40.5 °C	[1]
2	Increasing concentration	From 0.5% to 4%	Decreased from 45.9 to 41 °C	[1]
3	Adding PAA	Adding 4% PAA	Decreased from 45.9 to 35.4 °C	[1]
4	Adding LiCl	Adding 5 M LiCl	Decreased from 45 to 20 °C	[2]
5	Adding NaCl	Adding 0.7 M NaCl	Decreased from 43 to 31 °C	[3]
6	Adding PAA and adjust pH	Decreasing pH to 3.2	Decreased from 41 to 16 °C	[4]
7	Adding PAA-PAM	Distribute HPC into PAA-PAM matrix	Decreased from 45 to 30 °C	[5]

Table S2 Summary of previously reported information encryption hydrogels

Material platform	Methods used for introducing patterns	Stimuli	Color change	Investigation on mechanical properties	reference
PNIPAM-CDs hydrogel	Handwriting	UV light and temperature	Fluorescence	N.A.	6
PAM-Pho-CA hydrogels	Handwriting/mask	UV light	Fluorescence	N.A.	7
PAM-specific fluorophore	Assembly of hydrogel blocks with different fluorescent colors	UV light	Fluorescence	N.A.	8
PAM-lanthanide hydrogels	Assembly of hydrogel blocks with different fluorescent colors	UV light	Fluorescence	N.A.	9
P(VI-co-MAAc)-VPTP	Handwriting/mask	UV light	Fluorescence	N.A.	10
PAM hydrogel	Gel for covering pattern background	Solvent	Transmittance-opaque	N.A.	11
Cellulose Nanofibers-PNIPAM	Handwriting/mask	Solvent and temperature	Transmittance-opaque	N.A.	12
PAA-PMEA-organohydrogel	Handwriting/mask	solvent	Transmittance-opaque	N.A.	13
PDMA/PSM organogel	Photomasks	Solvent and temperature	Transmittance-opaque	N.A.	14
This work	3D printing	Temperature	Transmittance-opaque	Yes	

Reference

1 L. Zhang, H. Xia, F. Xia, Y. Du, Y. Wu and Y. Gao, *ACS Appl. Energy Mater.*, 2021, **4**, 9783–9791.

2 W. Guan, C. Lei, Y. Guo, W. Shi and G. Yu, *Adv. Mater.*, 2022, **2207786**, 1–6.

3 E. Weißenborn and B. Braunschweig, *Soft Matter*, 2019, **15**, 2876–2883.

4 X. Lu, Z. Hu and J. Schwartz, *Macromolecules*, 2002, **35**, 9164–9168.

5 Y. Niu, Y. Zhou, D. Du, X. Ouyang, Z. Yang, W. Lan, F. Fan, S. Zhao, Y. Liu, S. Chen, J. Li and Q. Xu, *Adv. Sci.*, 2022, **9**, 1–9.

6 C. D. P. N-isopropylacrylamide, .

7 N. Wang, K. K. Yu, K. Li, M. J. Li, X. Wei and X. Q. Yu, *ACS Appl. Mater. Interfaces*, 2020, **12**, 57686–57694.

8 X. Ji, R. T. Wu, L. Long, X. S. Ke, C. Guo, Y. J. Ghang, V. M. Lynch, F. Huang and J. L. Sessler, *Adv. Mater.*, 2018, **30**, 1–6.

9 Z. Li, H. Chen, B. Li, Y. Xie, X. Gong, X. Liu, H. Li and Y. Zhao, *Adv. Sci.*, 2019, **6**, 1–7.

10 C. N. Zhu, T. Bai, H. Wang, J. Ling, F. Huang, W. Hong, Q. Zheng and Z. L. Wu, *Adv. Mater.*, 2021, **33**, 1–8.

11 M. Li, H. Lu, X. Wang, Z. Wang, M. Pi, W. Cui and R. Ran, *Small*, 2022, **18**, 1–12.

12 Z. Chen, Y. Chen, Y. Guo, Z. Yang, H. Li and H. Liu, *Adv. Funct. Mater.*, , DOI:10.1002/adfm.202201009.

13 J. Liu, Z. Chen, Y. Chen, H. U. Rehman, Y. Guo, H. Li and H. Liu, *Adv. Funct. Mater.*, , DOI:10.1002/adfm.202101464.

14 F. Shan, X. Le, H. Shang, W. Xie, W. Sun and T. Chen, *ACS Appl. Mater. Interfaces*, 2023, **15**, 7405–7413.